Study of Vibrational Spectra of Interlayer Water in Sodium Beidellite by Molecular Dynamics Simulations

Satoru Suzuki* and Katsuyuki Kawamura†

Research Center for Deep Geological Environments, National Institute of Advanced Industrial Science and Technology, Higashi, Tsukuba, Ibaraki 305-8567, Japan

Received: May 24, 2004; In Final Form: June 30, 2004

To elucidate the molecular structure and water−clay interaction of interlayer water in sodium type smectite (hydrated layered alminosilicate), vibrational spectra of water were investigated using molecular dynamics (MD) simulations based on the free flexible force field model. Vibrational spectra of water were obtained by Fourier transformation of the velocity autocorrelation function of the hydrogen atom. Two distinct bands were found at 3365 and 3500 cm^{-1} in the stretching vibrational spectrum of interlayer water. The former band was assigned to an O−H bond unbound to the clay surface, while the latter was attributed to O−H vibrations bound to the clay surface through hydrogen bonding. The hydrogen bond distance (the H···O distance) between water and the clay surface ($H_{water}\cdots O_{clay} = 0.22$ nm) was larger than that between water molecules ($H_{water}\cdots O_{water} = 0.19$ nm). Detailed comparison of simulation results with IR spectroscopic observations indicated good agreement. The hydrogen bond structure and the vibrational spectrum of interlayer water suggest no rigid network structure of water molecules (icelike water) near the smectite surface.

1. Introduction

Properties of adsorbed water in the interlayer space of smectites (hereafter, "interlayer water") have attracted interests in clay science, colloid science, and soil science.[1−6] Because the vibrational frequency of the O−H bond is highly sensitive to the hydrogen bond strength with neighboring O atom(s) in many chemical compounds and hydrogen-bearing minerals,[7,8] the water molecule itself can be used as a molecular probe for the water−clay interaction. Infrared spectroscopy can be therefore employed to investigate the water−clay interaction.[3,4,6]

Two distinct IR absorption bands, one at 3400 cm^{-1} and the other at 3620 cm^{-1}, were reported for the typical interlayer water in smectite; however, comprehensive assignments of these bands were still lacking. Using the relationship between the vibrational frequency and hydrogen bond distance (O···O),[7] the hydrogen bond distance was estimated to be 0.28 nm for the 3400 cm^{-1} band and 0.30 nm for the 3620 cm^{-1} band assuming straight hydrogen bonding. Farmer and Russel[3] suggested that the hydrogen bond between the water and clay surface was ca. 0.30 nm. While this model was in accordance with the X-ray diffraction analysis of the hydrogen bond distance between the water and clay surface in Mg vermiculite, it was not confirmed in smectite because of no available structural information. In contrast, the 3400 cm^{-1} band is rarely assigned to O−H hydrogen-bonding with the clay surface.[6] The blue shift of the 3400 cm^{-1} band with increasing water content was considered due to the increase of the hydrogen bond distance between the water−clay surface.[6] However, these models, on the basis of the IR spectroscopy, were within the margin of interpretation. A comprehensive study of the water−clay interaction and the spectroscopic properties is needed.

We therefore investigated the relationships between the molecular structure and a vibrational spectrum of interlayer water in hydrated smectite by molecular dynamics (MD) simulation. The historical MD simulations of the hydrated smectite[9−14] were focused on the spatial distribution of water and ions or their self-diffusivities only. The MD simulation is also available to calculate the vibrational spectrum approximately identical to the IR spectrum. Because the positions of all atoms in the system were recorded during the simulation, we can compare the spectrum directly with the molecular structure without any interpretations.

In the present simulations, the free flexible potential model[12,13,15] was employed for water and clay because this potential model makes it possible to calculate a vibrational spectrum of water, which was impossible by a rigid molecule model such as "MCY" or "TIP4P".[9−11,14] The best approximation for interaction between water and the clay surface is validated by the vibrational properties of water because vibrational frequencies of hydroxyl groups are sensitive to hydrogen bonding. To discuss the relationships between these vibrational bands and the water−clay interaction, the hydrogen bonding (H···O distance) between water molecules or between water and the clay surface was investigated.

In the past decade, experimental[16] and ab initio MD simulation[17] studies have reported the two-dimensional network of adsorbed water (icelike water) on muscovite. Since the crystal structure of muscovite closely resembles that of smectite, such a strong network may exist for the hydrated smectite system. Using the results of MD simulations, we also examined the two-dimensional network of water on the surface of smectite.

2. Procedures

2.A. Outline of MD. MD simulations were carried out by the computer programs MXDTRICL and MXDORTOP.[18]

* To whom correspondence should be addressed. Present address: Nuclear Chemistry and Chemical Engineering Center (NUCEC), Institute of Research and Innovation, 1201 Takada, Kashiwa, Chiba, 277-0861, Japan. Phone: +81-4-7144-8972. Fax: +81-4-7144-7602. E-mail: kakusuzuki@iri.or.jp.

† Department of Earth and Planetary Sciences, Tokyo Institute of Technology, Ookayama 2-12-1, Meguro-ku, Tokyo 152-8551, Japan.

10.1021/jp047773k CCC: $27.50
Published on Web 08/11/2004

MXDTRICL (for single processing) was used to calculate the vibrational spectrum and molecular structure of interlayer water, while MXDORTOP (for parallel processing) was used for long simulation steps (200 000 steps). In these MD simulations, the motion of every atom in a system was solved by Newton's equation of motion. The velocity Verlet algorithm was used to solve the difference equations of motion.

The present simulations were carried out using the following interatomic potential model functions:[12,13,19−21]

$$u_{ij}(r_{ij}) = \frac{z_i z_j e^2}{4\pi\epsilon_0 r_{ij}} + f_0(b_i + b_j)\exp\left(\frac{a_i + a_j - r_{ij}}{b_i + b_j}\right) - \frac{c_i c_j}{r_{ij}^6} + D_{1ij}\exp(-\beta_{1ij} r_{ij}) + D_{2ij}\exp(-\beta_{2ij} r_{ij}) + D_{3ij}\exp[-\beta_{3ij}(r_{ij} - r_{ij}^*)^2] \quad (1)$$

$$u_{jik}(r_{ij}, r_{ik}, \theta_{jik}) = -f_k[\cos\{2(\theta_{jik} - \theta_0)\} - 1]\sqrt{k_j k_k} \quad (2.1)$$

$$k_j = \frac{1}{\exp\{g_r(r_{ij} - r_m)\} + 1} \quad (2.2)$$

Equation 1 represents the pair potential model. In this equation, the first and second terms on the right are the Coulomb energy term and a short-range repulsion energy term, respectively. r_{ij} is the distance between atoms i and j, z_i and z_j are the partial formal changes on atom i or j, respectively. e and ϵ_0 are the elementary electric charge and the permittivity of vacuum, respectively. f_0 (6.9511×10^{-11} N) is the constant for unit adaptations between the terms in eq 1. The third term in eq 1 represents the van der Waals interaction. The first to third terms were applied to every atom in a given system. The fourth to sixth terms correspond to the radial portion of covalent bonding. These terms were applied to Si−O, Al−O, and O−H bonds. Parameters a_i, b_i, c_i, D_{1ij}, D_{2ij}, D_{3ij}, b_{1ij}, b_{2ij}, b_{3ij}, and r_{ij}^* were optimized to reproduce the properties of the desired material described later. The three-body potential function (eq 2) was applied to H−O−H groups. This function corresponds to the angular portion of the covalent bond, representing the sp^3 hybrid orbital of the water molecule.[15] The parameters f_k, θ_0, g_r and r_m were optimized as described later. A periodic boundary condition was employed, and summation of the Coulomb energies and forces was executed using Ewald's method.

2.B. Clay Structure and Simulation Conditions. Smectite is a 2:1 layered aluminosilicate; each sheet consists of two tetrahedral silicate layers and one octahedral alumino layer with cations such as Na, K, Ca, or Mg located in the interlayer space. In the present study, MD simulations of sodium beidellite were performed with various amounts of interlayer water (Figure 1). The chemical formula for the simulated beidellite is indicated below:[22]

$$\text{simulated beidellite} = Na_{1/3}Al_2(Si_{11/3}Al_{1/3})O_{10}(OH)_2 \cdot nH_2O \quad (3)$$

Some of the Si atoms in a tetrahedral layer of beidellite are substituted by Al atoms, which causes charge deficit at this layer. An edge surface was not considered in the present simulations. A unit cell contains two clay sheets as shown in Figure 1 (72 molecules having the chemical formula given in eq 3). The number of water molecules n per formula will hereafter be referred to as "nH_2O system" or simply "n = the number of water molecules". The preparation of the initial beidellite structure has been described in detail elsewhere.[13]

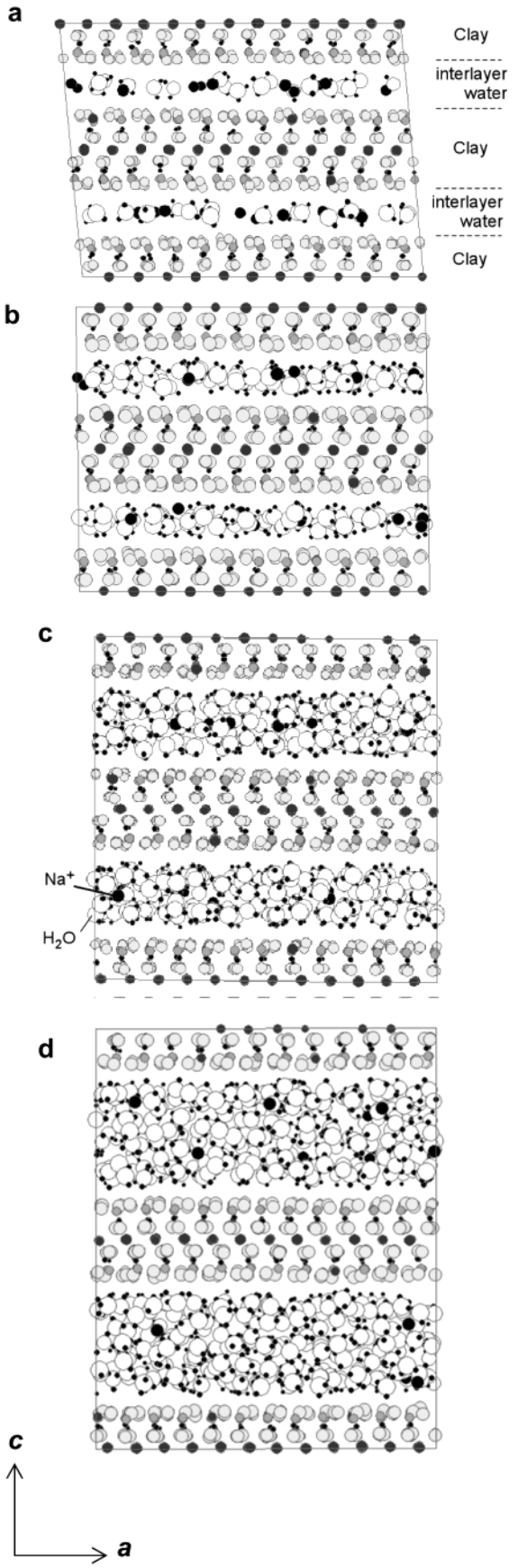

Figure 1. Snapshots of the Na beidellite cross section projected onto (010): (a) $n = 0.5$; (b) $n = 2.0$; (c) $n = 4.0$; (d) $n = 7.0$.

All Na, Si, Al, H, and O atoms of beidellite and the H and O atoms of a water molecule can move independently in all

TABLE 1: Potential Parameters Used in the Present Study (Version 03-01-11(0)[24])

ion	z_i [e]	m_i [g/mol]	a_i [Å]	b_i [Å]	c_i [(kcal/mol)$^{1/2}$/Å^3]
O	−1.271 94	16.0	1.887	0.148	29.6
Si	2.4	28.09	0.916	0.090	0
Al	2.25	26.98	1.022	0.080	0
Na	1	22.09	1.493	0.120	10
H	0.44	1.01	0.029	0.042	0
O (H_2O)	−0.92	16.0	1.7280	0.1275	23.88
H (H_2O)	0.46	1.01	0.0350	0.0440	0

covalent bond (radial)	D_{1ij} [kJ/mol]	β_{1ij} [1/Å]	D_{2ij} [kJ/mol]	β_{2ij} [1/Å]	D_{3ij} [kJ/mol]	β_{3ij} [1/Å]	r_{3ij} [Å]
Si−O	343 00	4	−3121	2			
Al−O	267 78	4	−1936	2			
H−O (clay)	214 11	7.7	−572	3.07	8.3	12.6	1.304
H−O (H_2O)	137 11	7.4	−523	3.13	8.3	12.8	1.283

covalent bond (angular)	f_k [10^{-19}J]	θ_{jik} [deg]	r_m [Å]	g_r [1/Å]
H−O−H (H_2O)	1.15	99.50	1.43	9.2

TABLE 2: Optimization Results of Bulk Water at 293 K and 0.1 MPa Together with Experimental Results

property	experiment	MD
density [g/cm^3]	0.997 [28]	0.996
self-diffusion coefficient [m^2/s]	2.2×10^{-9} [29]	1.4×10^{-9}
the first O−O distance [nm]	0.282 [30]	0.277
bending frequency [cm^{-1}]	1635[a]	1656
stretching frequency [cm^{-1}]	3330[a]	3322

[a] Determined in the presented study.

directions under the free flexible force field model. Table 1 lists the potential parameters indicated in eqs 1 and 2 used in the present study. The potential parameters for Si, Al, O, and H of the beidellite layer were optimized to a crystal structure of muscovite.[13] The parameters of interlayer Na were optimized in order to reproduce the NaCl crystal. This potential model yielded 0.26 nm of Na−OH_2 distance and 5−5.6 for the hydration number in NaCl solutions (NaCl concentration = 0.28 or 0.56 mol/dm^3 for a 2000 H_2O molecule system). These values were consistent with neutron scattering results for the Na−OH_2 distance and hydration number: 0.31 nm and 5.5−6.0, respectively.[23] Thus, the NaCl solution was successfully reproduced by the present model.

The potential parameters for O and H in water were optimized to the properties of bulk water or ice, e.g., the density, self-diffusivity, dielectric constant, lattice parameters of ice, or vibrational spectrum in the 253−373 K temperature range.[24] Table 2 lists optimization results at 293 K along with empirical results. A similar potential model has been used elsewhere.[12,13] However, in those studies, the dielectric constant of simulated bulk water was one-half of the empirical value. Thus, the reoptimized potential parameters[24] were used in the present paper. As a result, the difference between the empirical and simulation values of the dielectric constant of the bulk water was reduced to only several percent.[24] The vibrational spectrum of bulk water between them will be compared later.

The simulations were performed at a constant temperature of 293 K and a constant pressure (0.1 MPa: *NPT* ensemble). The time step was 0.4 fs. The thermal equilibrium of a system was confirmed by a preliminary MD simulation at each number of water per formula n with 50 000 steps, following which a regular simulation was done under the same conditions with 20 000 steps (8 ps) for calculations of the vibrational spectra or 200 000 steps (80 ps) for observations of atomic trajectory of interlayer water.

2.C. Analytical Method. The vibrational spectrum of interlayer water and the O−H bond of the octahedral layer were calculated by Fourier transformation of the velocity autocorrelation function of hydrogen,[15,25] according to Wiener−Khinchin's theorem.

$$\langle \mathbf{v}(t)\cdot\mathbf{v}(0)\rangle \equiv \frac{1}{N_s}\sum_{l=0}^{N_s-1}\frac{1}{N}\sum_{i=1}^{N} v_i(t+t_0+l\Delta\tau)\, v_i(t_0+l\Delta\tau) \quad (4)$$

where $v_i(t)$ is the velocity of the ith atom and N_s and $\Delta\tau$ are the number and interval of sampling, respectively. The nonpolarized spectrum was calculated from the averaged autocorrelation function of the three components of the velocity vector. When a polarized spectrum was calculated along the c axis, for example, the velocity autocorrelation function along c axis was used. Because the velocities of H atoms are recorded individually for interlayer water and O−H bond of the octahedral layer, each vibrational spectrum can be calculated separately as shown later.

A vibrational spectrum simulated in MD is approximately comparable to an IR spectrum. Spectral intensity simulated by MD represents "density of state (DOS)", whereas IR intensity is "absorbance" that is a product of DOS and molar absorptivity.[26] Molar absorptivity is proportional to the square of the first derivative of dipole moment μ at the equilibrium position ($d\mu/dr$). In the classical MD simulation, as the constant formal charge on atoms is assumed, the $d\mu/dr$ value is equal to the formal charge and so is constant. However, because electrons are distributed continuously between atoms in a real molecule, the $d\mu/dr$ value is variable depending on chemical environment. The spectral intensity simulated by MD therefore differs from IR absorbance.

The time average of the interatomic distances between the ith and jth atoms was calculated to obtain a pair correlation function $\langle n_{ij}(r)\rangle$:

$$\langle n_{ij}(r)\rangle = \frac{1}{\rho V N_s}\sum_{l=0}^{N_s-1}\frac{1}{N}\sum_{k=1}^{N} n_k(r, t_0+l\Delta\tau) \quad (5)$$

where $n_k(r, t_0 + l\Delta\tau)$ is the number of particles of the jth atom at a distance from the kth particle of the ith atom between $r - \Delta r/2$ and $r + \Delta r/2$ (Δr is 0.001 nm). ρ and V are the number of particles per unit volume and the volume of the shell between $r - \Delta r/2$ and $r + \Delta r/2$, respectively. N is the number of ith atom. N_s and $\Delta\tau$ are as defined in eq 4.

3. Results and Discussion

3.A. Simulation of Bulk Water. The present interatomic potential function and its parameters were optimized to represent various properties of bulk water and ice polymorphs. A detailed comparison between the simulations and empirical results is now in preparation elsewhere.[24] Thus, only a general outline is presented here.

Figure 2 shows the vibrational spectrum of bulk water simulated by the present potential model. The translational mode (0−300 cm^{-1}) of water molecules is mainly observed in the low-frequency region of the vibrational spectrum of O. The dynamics of H is a good approximation of intramolecular dynamics: librational (300−1000 cm^{-1}), bending (1500−1800 cm^{-1}), and stretching (3000−3700 cm^{-1}) modes of water. An IR spectrum experimentally obtained by the attenuated total reflectance (ATR) method is also shown in Figure 2. Owing to the experimental difficulties, the translational and librational

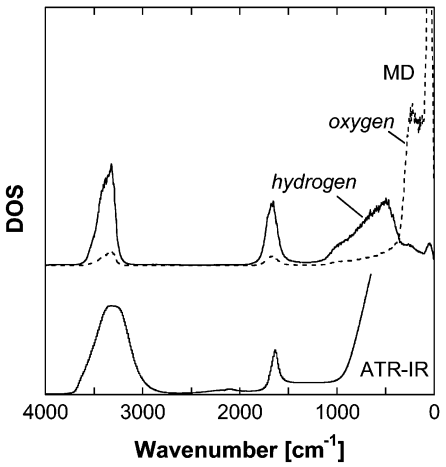

Figure 2. Vibrational spectra calculated from the velocity autocorrelation functions of oxygen and hydrogen atoms, shown together with an ATR-IR spectrum for bulk water.

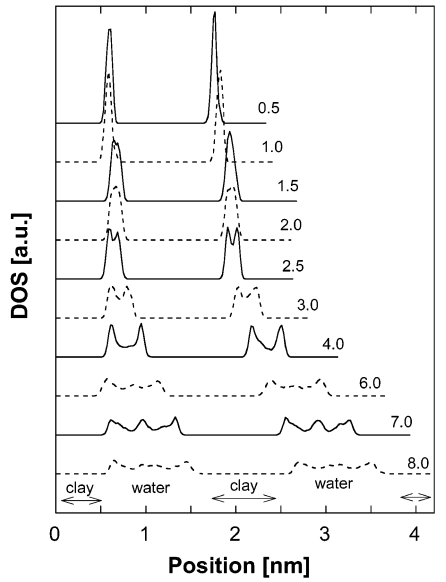

Figure 3. Spatial distribution of atoms along the *c* axis of beidellite. Distribution of water molecules is represented by the position of oxygen atoms. Two interlayer spaces among the three clay layers were contained in a unit cell. DOS: density of states.

modes were not observed in the IR spectrum. The frequencies of bending and stretching bands are compared in Table 2. The difference in vibrational frequency between the experimental and simulation result was several tens of cm^{-1}, which was considered acceptable.

3.B. Simulations of Hydrated Beidellite. Snapshots of hydrated beidellite at $n = 0.5$, 2.0, 4.0, and 7.0 are shown in Figure 1. All water molecules were located in the interlayer space. Figure 3 shows spatial distributions of water molecules along the *c* axis in two interlayer spaces of the unit cell (Figure 1). For the $n = 0.5-2.0$ systems, a single peak in each interlayer was observed. Each of these peaks was bifurcated in going from $n = 2.5$ to 4.0. At *n* values above 4.0, the peak was triplicate or more. The basal spacing $d_{(001)}$ of the simulated beidellite was plotted as a function of number of water *n* in Figure 4. The calculated $d_{(001)}$ coincided with the experimental results up to $n = 4.0$; however, they were largely different from each other above $n = 4.0$. This large difference in $d_{(001)}$ was found because all water molecules were forced to locate in the interlayer spaces in MD simulations. On the other hand, in the experimental system, the water can adsorb both interlayer space and the

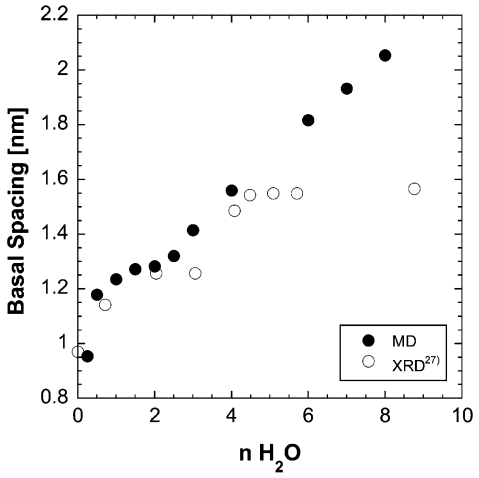

Figure 4. Basal spacing plotted as a function of *n*, number of water molecules.

external surface of the smectite particle. This external surface was not considered in the MD simulation. Because the water molecules presumably adsorbed on the external surface above $n = 4.0$, the increase in $d_{(001)}$ was not observed experimentally.

Comparing Figures 3 and 4, the basal spacing $d_{(001)}$ of 1.2−1.3 nm corresponds to the single water layer, while $d_{(001)}$ of 1.3−1.56 nm corresponds to the double layers and $d_{(001)} > 1.55$ nm corresponds to triple or more layers. The arrangement of a typical water layer, namely, singlet ($n = 0.5$ and 2.0), doublet ($n = 4.0$), or triplet ($n = 7.0$), will be further analyzed. Because the vibrational frequency of the hydroxyl bond in hydrous compounds is correlated with the hydrogen bond distance,[7] the pair correlation functions (PCF) between H and O of hydrated beidellite were calculated (Figure 5). Figure 5a shows the PCFs between the H and O of interlayer water (denoted by H_{water} and O_{water}, respectively). The strong peak at 0.098 nm was attributed to intramolecular O−H bonds, while the other peaks were due to intermolecular O···H bond (hydrogen bonding). At $n = 2.0$, 4.0, and 7.0, a secondary peak was observed at 0.188 nm; the exact same peak was observed in the case of bulk water, indicating the presence of hydrogen bonding in interlayer water. On the other hand, no peak was found at 0.188 nm for $n = 0.5$; i.e., no hydrogen bonding occurred in this case.

Figure 5b shows the PCFs of the oxygen in clay (denoted by O_{clay}) and H_{water} that represent the water−clay interaction. The first nearest peak was found at around 0.22 nm, and this $O_{clay}-H_{water}$ distance was longer than the $O_{water}-H_{water}$ one. This indicated that the hydrogen bonding between clay and the water molecule was weaker than that between water molecules. On the other hand, pair correlation functions between O_{water} and the H atoms in the octahedral layer of clay (denoted by H_{clay}) revealed the absence of hydrogen bonding because the nearest peak was found at around 0.40−0.43 nm (Figure 5c).

Figure 6a shows the inclination angle distribution of the dipole axis of water molecules located within 0.3 nm from the smectite surface with respect to the *c* axis. The peak top of the distribution shifted from 90° ($n = 0.5$, 1.0) to 60° ($n = 1.5-7.0$). This indicates that one of the O−H bonds of the water molecule was inclined at 35° with respect to the *c* axis in the $n = 0.5$ system and then became approximately parallel to the *c* axis at $n = 2.0-7.0$, as shown in Figure 7. This preferred orientation was significant for the water molecules next to the clay surface, and no clear orientation was found around the center of the interlayer, for example, in the $n = 7.0$ system (Figure 6b). These observations agreed with results of studies[11] using the rigid water and clay model, demonstrating the reliability of our model.

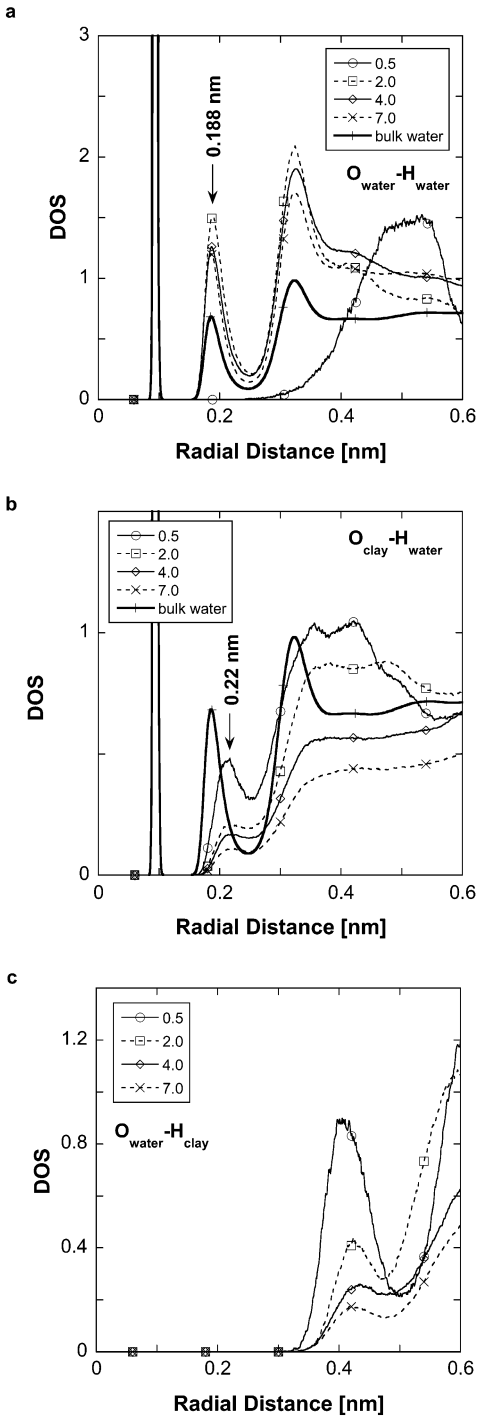

Figure 5. Pair correlation function of oxygen and hydrogen for the $n = 0.5$, 2.0, 4.0, and 7.0 systems: (a) $H_{water}-O_{water}$; (b) $H_{clay}-O_{water}$; (c) $H_{water}-O_{clay}$.

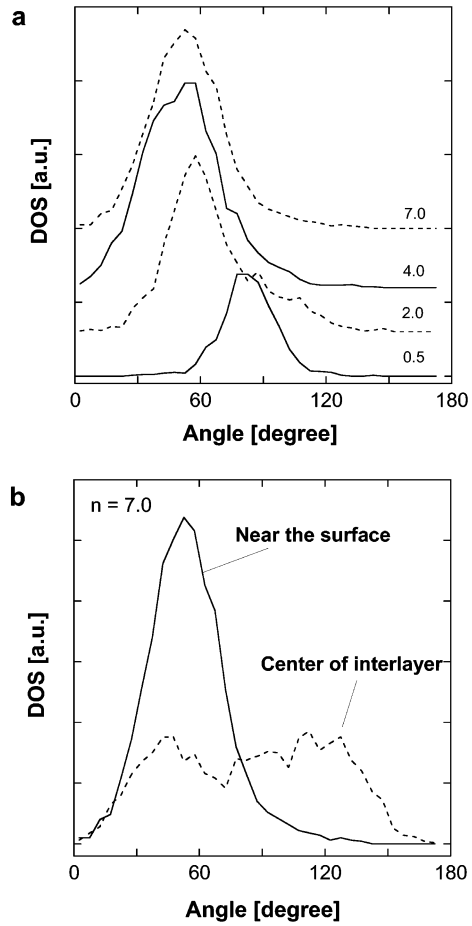

Figure 6. Histograms of inclination angle of dipole axis of H_2O with respect to the normal vector to the beidellite surface: (a) water molecules next to the surface in the $n = 0.5$, 2.5, 4.0, and 7.0 systems; (b) water molecules next to the surface (solid line) and unbound water at the center of interlayer water (broken line) in the $n = 7.0$ system.

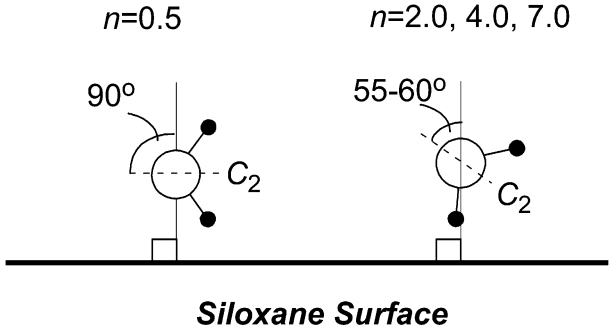

Figure 7. Schematic of orientation of water molecule.

The molecular structure of interlayer water affected its vibrational spectrum. Figure 8a shows the vibrational spectra of interlayer water for the $n = 0.5$, 2.0, 4.0, and 7.0 systems. The stretching vibrational bands were observed at around 3500 cm^{-1} for $n = 0.5$, while at $n = 2.0$ and 4.0, the stretching band was bifurcated into peaks at 3365 and 3500 cm^{-1}. At $n = 7.0$, the stretching band shape and frequency became similar to those of bulk water.

With the preferred orientation of the water molecule determined (Figure 6), polarized spectra were calculated to assign the vibrational band. Figure 9a shows vibrational spectra of interlayer water along the *c* axis of clay and along the *a* and *b* axes (*ab* plane) of clay at $n = 2.0$, along with a nonpolarized spectrum. The 3500 cm^{-1} band was dominant along the *c* axis, while the 3365 cm^{-1} band was dominant along the *ab* plane. In the $n = 2.0$ system, hydrogen bonding between water molecules was observed only along the *ab* plane, while that between water and clay surface was directed along the *c*-axis of clay because of the 2-D distribution of interlayer water (Figure 9b). Therefore, the 3365 cm^{-1} band was attributed to hydrogen bonding between water molecules, while the 3500 cm^{-1} band was assigned to hydrogen bonding between interlayer water and the clay surface. These assignments were corroborated by the relationship between the vibrational frequency of the O−H bond and the hydrogen bond distance.[7] As shown in parts a and b of Figure 5, the hydrogen bond distance defined as the $H_{water}-O_{clay}$ distance (ca. 0.22 nm) was longer than the $H_{water}-O_{water}$ distance (ca. 0.188 nm). With increasing *n*, the intensity of the 3365

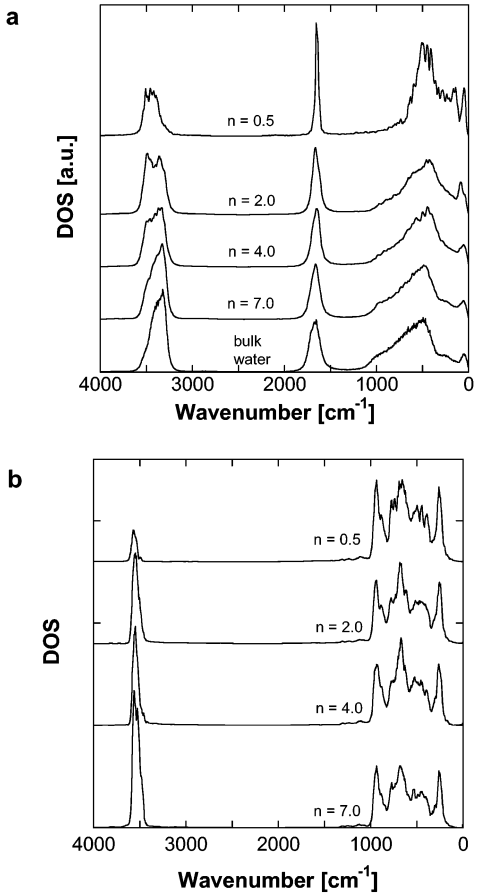

Figure 8. (a) Vibrational spectra of interlayer water in the $n = 0.5$, 2.0, 4.0, and 7.0 systems, shown together with that of bulk water. (b) O−H bond at octahedral layer.

cm^{-1} band increased relative to the 3500 cm^{-1} band and apparently disappeared at $n = 7.0$ (Figure 8). Given that the water molecule next to the clay surface was still oriented at high n values (Figure 6), the disappearance of the 3500 cm^{-1} band was due to the increase of the unbound water fraction against the fraction of bound water near the clay surface.

The vibrational spectrum of the octahedral O−H bond is shown in Figure 8b. The stretching band found at 3560 cm^{-1} did not vary with the n value. This was due to absence of hydrogen bond between the octahedral O−H bond and interlayer water, as shown in Figure 5c. A spectral intensity of stretching mode at $n = 0.5$ was smaller than those at $n = 2.0-7.0$. Because the spectral intensity was normalized by the integrated intensity from 0 to 4000 cm^{-1}, this is not due to any difference in amount or orientation of the O−H bond between systems. A more detailed discussion is out of the scope of the present paper.

These simulation results were compared with an IR spectrum of interlayer water.[3,6] Farmer and Russell[3] performed the IR measurements by using the self-supporting, oriented film of smectite and vermiculite. To obtain the IR spectrum of interlayer water, water (H_2O) was exchanged by deuterated water (D_2O). Famer and Russel found two distinct peaks at ca. 2690 and 2500 cm^{-1} of D_2O, which correspond to the 3500 and 3365 cm^{-1} bands of interlayer water (H_2O) in the MD simulation, respectively. Because the intensity of the 2690 cm^{-1} band increased with decreasing incidence angle of the IR beam, the 2690 cm^{-1} band was taken to suggest that the O−D bond of interlayer water was directed toward the clay surface. The $O_{clay}-O_{H2O}$ distance was estimated to be 0.28−0.29 nm by Farmer and Russell. The $O_{clay}-O_{H2O}$ distance instead of the $H_{water}-O_{clay}$ distance in

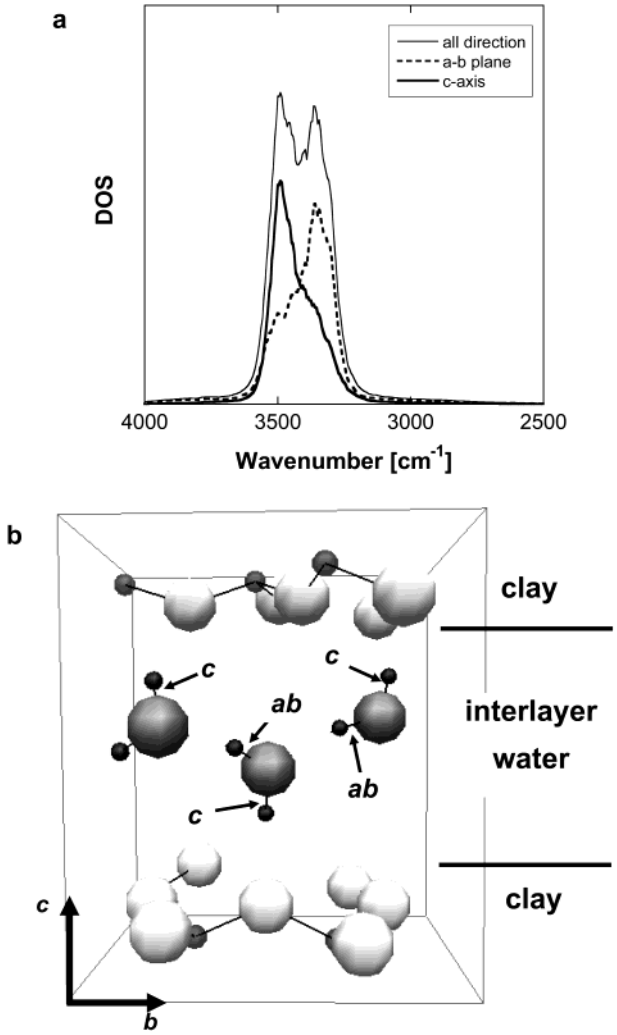

Figure 9. (a) Polarized spectra of interlayer water in the $n = 2.0$ system. (b) Snapshot of interlayer water and the smectite surface ($n = 2.0$ system). "ab" and "c" indicate the O−H bond directed along the *ab* plane and the *c* axis of clay, respectively.

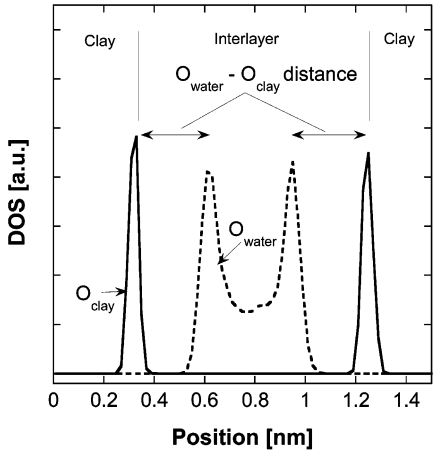

Figure 10. The $O_{clay}-O_{H2O}$ distance was determined as the distance between peak tops of O_{clay} and O_{H2O} distributions.

Figure 5b was determined to be 0.32 nm as shown in Figure 10. Thus, our MD simulation quantitatively confirmed the water−clay interaction model experimentally suggested.[3] On the other hand, the blue shift of 3400 cm^{-1} [6] band was probably due to an increase in the hydrogen bond distance between water molecules, based on our band assignments above. The 3400 cm^{-1} band was attributed to the water−water hydrogen bond.

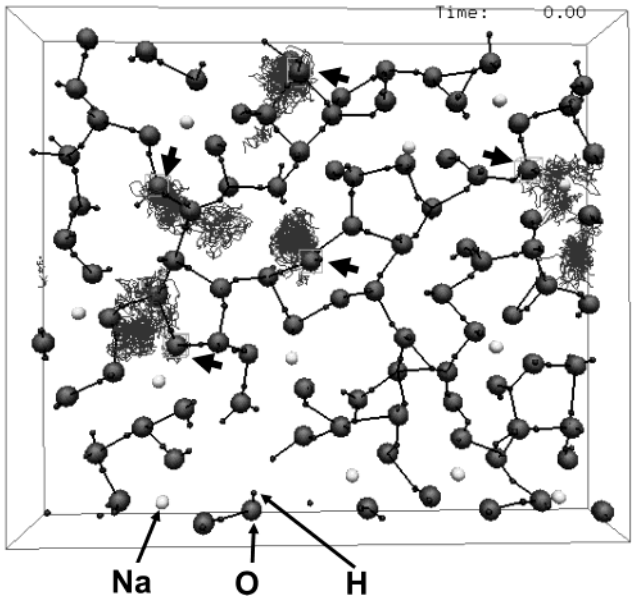

Figure 11. Snapshot of interlayer water next to a clay surface in the $n = 4.0$ system projected onto the c axis of clay. Chemical bonds were drawn for interatomic distances of less than 0.20 nm, which is the typical hydrogen bond distance in bulk water. Atomic trajectories were drawn for oxygen atoms of several water molecules, indicated by bold arrows.

3.C. Two-Dimensional Structure of Interlayer Water. The experimental and simulation studies reported the two-dimensional network of adsorbed water (icelike water) on muscovite whose crystal structure was similar to that of smectite. Therefore, we investigated the presence of this water network on the smectite surface by our MD simulations. Figure 11 shows the network structure of interlayer water next to the clay surface in the $n = 4.0$ system. Hydrogen bonds between water molecules are indicated by solid lines when the H−O distance is less than 0.20 nm. The trajectories were drawn for oxygen atoms indicated by bold arrows in 80 ps (200 000 steps). Although water molecules were strongly oriented to the clay surface (Figure 6), they could diffuse and their network structure was varied with time. Thus, no stable icelike structure of adsorbed water was found in the interlayer water of smectites, which disagreed with existing data on muscovite.[17] This contradiction was probably due to the ordered structure of interlayer cation and the smaller layer charge of smectite ($-0.33e$) compared with that of muscovite ($-1.0e$). Because potassium as interlayer cation for muscovite[17] was located as inner-sphere complexes whose distribution was ordered, adsorbed water molecules possibly formed a well-ordered 2-D structure. If potassium was disordered, the network structure may be strained because of the hydration of cations. In the presented simulations, Na was randomly distributed and diffusible during the simulation (Figure 11). The lower layer charge of smectite caused a weaker water−mineral surface interaction. Hence, the molecular structure of interlayer water was presumably not affected by the surface structure of smectite. The rigid icelike structure of interlayer water was thus concluded to be unfavorable in hydrated smectite.

The simulated vibrational spectrum of Na beidellite agreed well with the experimental spectrum, demonstrating the reliability of our water−clay interaction model. This interaction model allows us to calculate more reliably the other properties of interlayer water: density, diffusivity, viscosity, hydration of cations, etc. This model therefore provides appropriate data with scientific soundness for engineering applications such as use of a clay barrier for radioactive waste.[12]

The vibrational frequency of interlayer water experimentally depended on the exchangeable cation and/or the charge deficit layer. The same MD simulations for Na montmorillonite (charge deficit occurred at the octahedral layer due to the $Al^{3+} \Leftrightarrow Mg^{2+}$ substitution) showed the two distinct bands at approximately the same position as Na beidellite (unpublished data). Despite the absence of a hydrogen bond between the octahedral O−H bonds and interlayer water, the vibrational spectrum was affected by the number of water molecules. Detailed investigations are needed to clarify the influence of cation, distribution of charge deficit, and the nature of octahedral O−H bonds.

Acknowledgment. The authors acknowledge Dr. H. Sato for discussions on the results presented, and Dr. Y. Nakashima, Dr. I. McKinley, and Dr. L. McKinkey for critical review of the draft manuscript. The authors thank the anonymous referees for constructive comments and suggestions.

References and Notes

(1) Sposito, G.; Prost, R. *Chem. Rev.* **1982**, *82*, 553.
(2) Woessner, D. E.; Snowden, B. S., Jr. *J. Colloid Interface Sci.* **1969**, *30*, 54.
(3) Farmer, V. C.; Russell, J. D. *Trans. Faraday Soc.* **1971**, *67*, 2737.
(4) Prost, R. *Ann. Agron.* **1975**, *26*, 463.
(5) Mamy, J. *Ann. Agron.* **1968**, *19*, 175.
(6) Xu, W. C.; Johnston, T.; Parker, P.; Agnew, S. F. *Clays Clay Miner.* **2000**, *48*, 120.
(7) Nakamoto, K.; Margoshes, M.; Rundle, R. E. *J. Am. Chem. Soc.* **1955**, *77*, 6480.
(8) Aines, R. D.; Rossman, G. R. *J. Geophys. Res.* **1984**, *89*, 4059.
(9) Refson, K.; Skipper, N. T.; McConnell, D. C. *Geochemistry of Clay Pore Fluid Interactions*; Chapman & Hall: London, 1993; p 62.
(10) Skipper, N. T.; Refson, K.; McConnell, D. C. *Geochemistry of Clay Pore Fluid Interactions*; Chapman & Hall: London, 1993; p 40.
(11) Chang, F.-R. C.; Skipper, N. T.; Sposito, G. *Langmuir* **1995**, *11*, 2734.
(12) Ichikawa, Y.; Kawamura, K.; Nakano, M.; Kitayama, K.; Kawamura, H. *Eng. Geol.* **1999**, *54*, 21.
(13) Kawamura, K.; Ichikawa, Y. *Bull. Earthquake Res. Inst., Univer. Tokyo* **2001**, *76*, 311.
(14) Marry, V.; Turq, P.; Cartailler, T.; Levesque, D. *J. Chem. Phys.* **2002**, *117*, 3454.
(15) Kumagai, N.; Kawamura, K.; Yokokawa, T. *Mol. Simul.* **1994**, *12*, 177.
(16) Hu, J.; Xiao, X.-D.; Ogletree, D. F.; Salmeron, M. *Science* **1995**, *268*, 267.
(17) Odelius, M.; Bernasconi, M.; Parrinello, M. *Phys. Rev. Lett.* **1997**, *78*, 2855.
(18) MD simulation programs MXDTRICL and MXDORTOP were written by K. Kawamura. Details are found in refs 14, 15, and 19−21 and references therein.
(19) Sato, H.; Yamagishi, A.; Kawamura, K. *J. Phys. Chem. B.* **2001**, *105*, 7990.
(20) Tamura, K.; Kawamura, K. *J. Phys. Chem. B* **2002**, *196*, 271.
(21) Sakuma, H.; Tsuchiya, T.; Kawamura, K.; Otsuki, K. *Surf. Sci.* **2003**, *536*, L396.
(22) Strunz, H.; Nickel, E. H. *Strunz Mineralogical Tables: Chemical−Structural Mineral Classification System*, 9th ed.; Schweizebart, 2001.
(23) Ohtaki, H.; Radnai, T. *Chem. Rev.* **1993**, *93*, 1157.
(24) Kawamura, K. Manuscript in preparation.
(25) Itoh, H.; Kawamura, K.; Hondoh, T.; Mae, S. *J. Chem. Phys.* **1998**, *109*, 4894.
(26) Hollas, J. M. *Modern Spectroscopy*, 3rd ed.; John Wiley & Sons: New York, 1996.
(27) Fu, M. H.; Zhang, Z. Z.; Low; P. F. *Clays Clay Miner.* **1990**, *38*, 485.
(28) *Handbook of Chemistry: Pure Chemistry*, 4th ed.; Maruzen, 1993.
(29) Mills, R. *J. Phys. Chem.* **1973**, *77*, 685.
(30) Narten, A. H.; Danford, M. D.; Levy, H. A. *Discuss. Faraday Soc.* **1969**, *43*, 97.